

Isoprenoid Biosynthesis Inhibitors Targeting Bacterial Cell Growth

Janish Desai⁺,^[a] Yang Wang⁺,^[b] Ke Wang,^[b] Satish R. Malwal,^[b] and Eric Oldfield^{*,[a, b]}

We synthesized potential inhibitors of farnesyl diphosphate synthase (FPPS), undecaprenyl diphosphate synthase (UPPS), or undecaprenyl diphosphate phosphatase (UPPP), and tested them in bacterial cell growth and enzyme inhibition assays. The most active compounds were found to be bisphosphonates with electron-withdrawing aryl-alkyl side chains which inhibited the growth of Gram-negative bacteria (*Acinetobacter baumannii*, *Klebsiella pneumoniae*, *Escherichia coli*, and *Pseudomonas aeruginosa*) at $\sim 1\text{--}4\ \mu\text{g mL}^{-1}$ levels. They were found to be potent inhibitors of FPPS; cell growth was partially "res-

cued" by the addition of farnesol or overexpression of FPPS, and there was synergistic activity with known isoprenoid biosynthesis pathway inhibitors. Lipophilic hydroxyalkyl phosphonic acids inhibited UPPS and UPPP at micromolar levels; they were active ($\sim 2\text{--}6\ \mu\text{g mL}^{-1}$) against Gram-positive but not Gram-negative organisms, and again exhibited synergistic activity with cell wall biosynthesis inhibitors, but only indifferent effects with other inhibitors. The results are of interest because they describe novel inhibitors of FPPS, UPPS, and UPPP with cell growth inhibitory activities as low as $\sim 1\text{--}2\ \mu\text{g mL}^{-1}$.

Introduction

The emergence of resistance to antibiotics is a public health threat,^[1] so new drugs and new drug leads that act on new targets are of interest.^[2] Many of the antibiotics which, over time, have been of particular importance inhibit enzymes involved in bacterial cell wall biosynthesis; therefore, this is a potentially important area for drug discovery. Bacterial cell wall biosynthesis involves many enzymes. Initially, dimethylallyl diphosphate (DMAPP, **1**) and isopentenyl diphosphate (IPP, **2**) are produced by the 2-C-methyl-D-erythritol-4-phosphate or mevalonate pathways (Figure 1). In most bacteria, DMAPP then reacts sequentially with two IPP molecules to form *trans*-farnesyl diphosphate (FPP, **3**) in a reaction catalyzed by FPP synthase (FPPS). FPP then acts as the substrate for undecaprenyl diphosphate synthase (UPPS) to form the C₅₅ isoprenoid, undecaprenyl diphosphate (UPP, **4**). UPP is hydrolyzed by UPP phosphatase (UPPP) to form undecaprenyl phosphate (UP, **5**), which is then used (in most bacteria) for peptidoglycan, lipopolysaccharide, and wall teichoic acid biosynthesis. FPPS, UPPS, and UPPP are thus of interest as targets for novel anti-infective agents. In mycobacteria, cell wall biosynthesis is different; it begins with the formation of *cis*-FPP, not *trans*-FPP, followed by formation

of *cis*-decaprenyl (not undecaprenyl) diphosphate, and is not discussed further here.

Our research group previously reported the lipophilic bisphosphonate **6** to have modest activity against *E. coli* (IC₅₀ $\sim 30\ \mu\text{M}$)^[3] and to exhibit potent synergy (fractional inhibitory concentration index, FICI = 0.18) with fosmidomycin (**7**), which inhibits the MEP pathway (Figure 2).^[4] We also reported several benzoic acids, as well as diamidines such as **8**, to inhibit UPPS, and compound **8** was found to act synergistically with methicillin against methicillin-resistant *Staphylococcus aureus* (MRSA).^[5] Compound **8** was also active *in vivo* in a mouse model of infection. We also found that the fertility drug clomiphene (**9**) is a UPPS inhibitor,^[6] as well as an uncoupler of oxidative phosphorylation;^[7] the two effects presumably contribute to cell growth inhibition. In this study, we synthesized and tested a series of bisphosphonates, phosphonates, and carboxylic acids and tested them for prenyl synthase activity and for activity against both Gram-positive and Gram-negative bacteria.

Results and Discussion

Farnesyl diphosphate synthase as an antibacterial target

FPPS is the target for bisphosphonate bone resorption drugs such as zoledronate (**10**), though **10** has essentially no antibacterial activity. However, as noted above, in earlier work^[3] we found that the lipophilic bisphosphonate **6** (an FPPS inhibitor first made by Widler et al.^[8] as a potential bone resorption drug) had weak but measurable ($\sim 30\ \mu\text{M}$) activity against the Gram-negative bacterium *E. coli*. We also found activity against FPPS from the trypanosomatid parasite *Trypanosoma brucei* (TbFPPS) and we solved the X-ray crystallographic structure of

[a] J. Desai,⁺ Prof. E. Oldfield
Center for Biophysics and Quantitative Biology,
University of Illinois at Urbana-Champaign,
1110 West Green Street, Urbana, IL 61801 (USA)
E-mail: eo@chad.scs.uiuc.edu

[b] Dr. Y. Wang,⁺ Dr. K. Wang, Dr. S. R. Malwal, Prof. E. Oldfield
Department of Chemistry,
University of Illinois at Urbana-Champaign,
600 South Mathews Avenue, Urbana, IL 61801 (USA)

[*] These authors contributed equally to this work.

Supporting information and the ORCID identification number(s) for the author(s) of this article can be found under <http://dx.doi.org/10.1002/cmdc.201600343>.

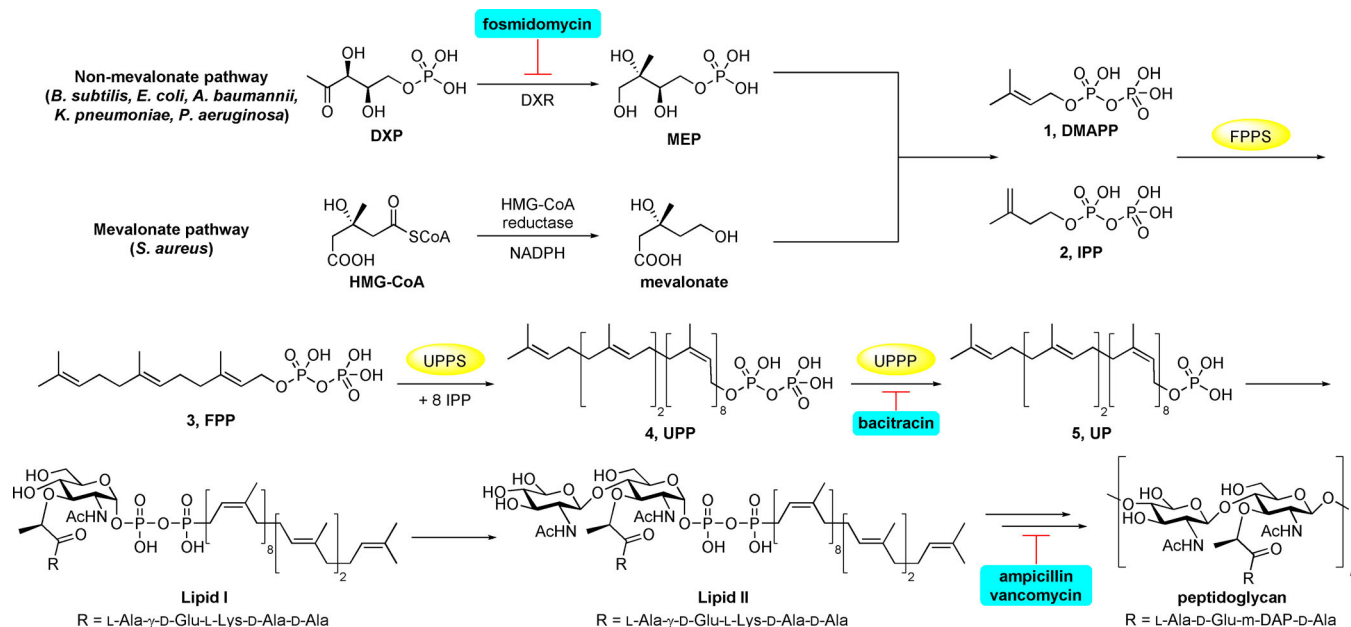


Figure 1. Illustration of selected molecules involved in cell wall biosynthesis in most bacteria. Also shown are sites of action of some antibiotics and potential targets, discussed in the text.

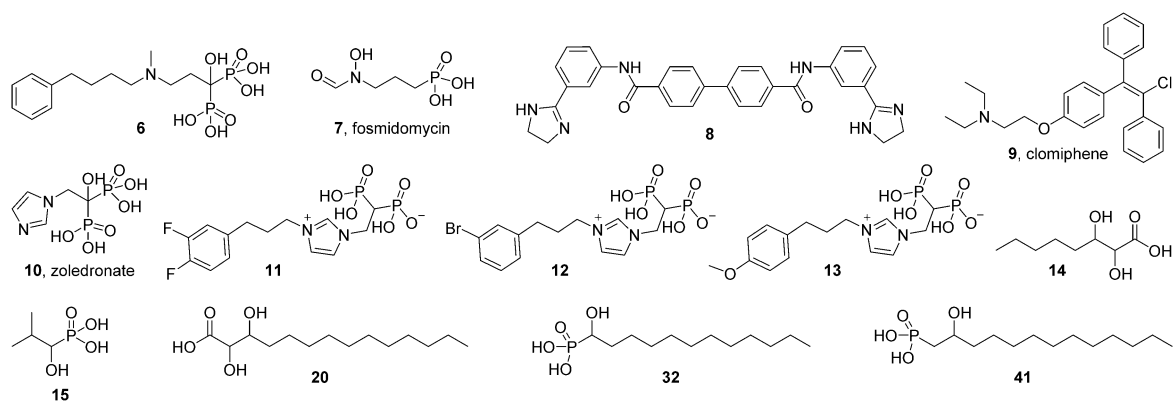


Figure 2. Structures of substrates and inhibitors discussed in the text.

a TbFPPS-6 complex.^[9] Interestingly, the crystal structure showed the phenyl group in **6** to be close ($\sim 4 \text{ \AA}$) to a tyrosine residue (Y99), which in human FPPS (HsFPPS) is phenylalanine (F99). This Phe residue in HsFPPS is thought to be involved in limiting chain elongation to C_{15} and is present in FPPS isoforms from other eukaryotes such as that from *Schistosoma mansoni*.^[10] A partial alignment of TbFPPS, HsFPPS, SmFPPS, as well as Gram-positive and Gram-negative bacterial FPPSs (*S. aureus*, *Bacillus subtilis*, *E. coli*, *Acinetobacter baumannii*, *Klebsiella pneumoniae*, and *Pseudomonas aeruginosa*) is shown in Figure 3.

The bacterial FPPSs are different from those of eukaryotes in that there are two extra amino acids in the first aspartate-rich motif (FARM, which is involved in catalysis), plus, there is a conserved YS sequence: both motifs are highlighted in yellow in Figure 3. In our earlier work we found that longer- or shorter-chain analogues of **6** had less activity than **6** against FPPS and *E. coli* cell growth.^[3] Also, based on structure alignments (dis-

cussed more below), it appeared that the aromatic group in **6** (or its analogues) might interact with the electron-rich Tyr in the bacterial YS motif. We thus hypothesized that it might be possible to obtain improved activity by incorporating electron-withdrawing substituents on the phenyl group in **6** or its analogues, leading to a tyrosine-inhibitor charge-transfer interaction. In contrast, the addition of an electron-donating substituent might decrease activity, basically as we suggested in earlier work on bisphosphonate inhibitors of ATP-mediated HIV-1 reverse transcriptase catalyzed excision of chain-terminating 3'-azido-3'-deoxythymidine.^[11] We therefore made three analogues of **6**, compounds **11–13**, and tested them against various FPPSs as well as in bacterial cell growth inhibition assays.

As can be seen in Figure 2, in addition to adding substituents (difluoro, bromo or methoxy) to the phenyl group, we replaced the amine with an imidazolium group, as in other work^[12] we found such species to be potent FPPS inhibitors

		FARM											SARM											
TbFPPS	96-	Q	A	H	Y	L	V	E	D	D	I	-	-	M	D	N	S		255-	D	D	V	M	D
HsFPPS	96-	Q	A	F	F	L	V	A	D	D	I	-	-	M	D	S	S		243-	D	D	Y	L	D
SmFPPS	94-	H	A	G	F	L	V	L	D	D	I	-	-	I	D	N	S		271-	D	D	Y	L	D
SaFPPS	75-	H	T	Y	S	L	I	H	D	D	L	P	A	M	D	N	D		218-	D	D	L	L	D
BsFPPS	78-	H	T	Y	S	L	I	H	D	D	L	P	C	M	D	D	D		223-	D	D	I	L	D
EcFPPS	77-	H	A	Y	S	L	I	H	D	D	L	P	A	M	D	D	D		223-	D	D	I	L	D
AbFPPS	82-	H	C	Y	S	L	A	H	D	D	L	P	C	M	D	N	D		230-	D	D	I	L	D
KpFPPS	77-	H	A	Y	S	L	M	H	D	D	L	P	A	M	D	D	D		223-	D	D	I	L	D
PaFPPS	77-	H	A	Y	S	L	V	H	D	D	L	P	A	M	D	D	D		218-	D	D	I	L	D

Figure 3. ClustalW alignments of *T. brucei*, human, *S. mansoni*, and six bacterial FPPSs. The YS pair is present in all of the bacterial FPPSs, and the Tyr residue is proposed here to interact with electron-deficient aryl groups in bisphosphonate inhibitors. FARM = first aspartate-rich motif; SARM = second aspartate-rich motif; wavy lines represent residues omitted from the alignment, for clarity.

with good in vivo activity. Moreover, we replaced the 1-OH group with 1-H because the hydroxy group is involved (in other bisphosphonates) in potent bone binding.^[13] These analogues also appeared to be more readily synthesized than the corresponding amines. We then tested all three compounds against FPPSs from *E. coli*, *P. aeruginosa*, *T. brucei*, *H. sapiens*, and *S. mansoni*, as well as against human geranylgeranyl diphosphate synthase (HsGGPPS). The results are shown in Table 1 and Figure S1. As can be seen in Table 1, two of the three bisphosphonates had activity in the ~70–600 nM range against EcFPPS, PaFPPS, TbFPPS, HsFPPS, SmFPPS, and HsGGPPS, generally similar to that observed (under the same assay conditions) with zoledronate, although zoledronate is only a weak HsGGPPS inhibitor,^[12] whereas **11–13** are all active, consistent with previous work on other lipophilic bisphosphonates.

However, with the two bacterial enzymes EcFPPS and PaFPPS, there is essentially no FPPS inhibition by the methoxy

analogue **13**. This behavior was originally predicted, so the differences between the EcFPPS/PaFPPS and other FPPS inhibition results with compounds **11–13** may be due to interactions with a Tyr residue (Y79), in addition to small differences between the type II (EcFPPS; eubacterial) and type I (eukaryotic) FPPS structures. At present, we do not have the structures of **11**, **12**, or **13** bound to a bacterial FPPS. However, Figure 4

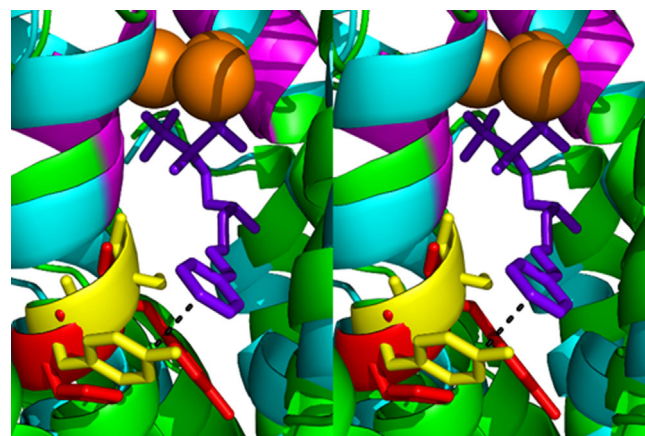


Figure 4. Stereo representation of superimposition of TbFPPS-6 (PDB ID: 2P1C) with EcFPPS (PDB ID: 1RQJ). The side chains of HY (red) and YS (yellow) amino acids are shown in stick format, compound **6** is shown in purple, the first aspartate-rich motif (FARM) is shown in magenta, and Mg²⁺ ions are shown as orange spheres.

shows a stereo structural alignment of TbFPPS-6 (PDB ID: 2P1C) with EcFPPS (PDB ID: 1RQJ) from which it can be seen that the conserved YS residues in EcFPPS could align with the (electron-rich) Tyr in close proximity (~3 Å) to the phenyl group in the TbFPPS-6 structure, consistent with a role for a charge-transfer interaction^[11] with inhibitors with electron-withdrawing phenyl substituents. This is a hypothesis, of course, but clearly there are major differences in FPPS inhibition between **11**, **12**, and **13** in the bacterial and eukaryotic

Enzymes/ Organisms	11	12	13
EcFPPS	0.12 ± 0.025	1.6 ± 0.28	> 100
PaFPPS	0.32 ± 0.068	0.58 ± 0.15	> 100
TbFPPS	0.12 ± 0.026	0.16 ± 0.029	0.51 ± 0.20
HsFPPS	0.065 ± 0.012	0.12 ± 0.026	0.084 ± 0.0083
SmFPPS	0.57 ± 0.11	0.33 ± 0.054	0.50 ± 0.065
HsGGPPS	0.39 ± 0.073	0.33 ± 0.089	0.53 ± 0.11
<i>S. aureus</i>	> 100	> 100	> 100
<i>B. subtilis</i>	39 ± 13	26 ± 5.9	> 100
<i>M. smegmatis</i>	6.8 ± 3.0	7.5 ± 2.4	20 ± 5.3
<i>E. coli</i>	2.1 ± 0.57	1.7 ± 0.38	> 100
<i>A. baumannii</i>	2.8 ± 0.70	2.0 ± 0.50	> 100
<i>K. pneumonia</i>	2.3 ± 0.49	2.4 ± 0.43	> 100
<i>P. aeruginosa</i>	3.5 ± 0.78	3.3 ± 0.68	> 100
HEK293	27 ± 4.0	36 ± 8.6	82 ± 22

[a] Data are the mean ± SD for duplicate experiments.

systems, and charge transfer seems a likely reason for the differences observed.

We next tested **11–13** in cell growth inhibition assays: first against the Gram-positives *S. aureus* and *B. subtilis*, as well as *Mycobacterium smegmatis*, second against the Gram-negatives *E. coli*, *P. aeruginosa*, *K. pneumoniae* and *A. baumannii*, and third against a human embryonic kidney cell line (HEK293). Results are shown in Table 1 and Figures S2 and S3. There was little or no activity of **11–13** against *S. aureus* or *B. subtilis*, but there was some activity against *M. smegmatis* (corresponding to an IC_{50} value of $\sim 7 \mu\text{g mL}^{-1}$ for **11** and **12**). However, the difluoro species **11** as well as the bromo species **12** had promising activity against all four Gram-negative bacteria in the $\sim 1\text{--}4 \mu\text{g mL}^{-1}$ range, but the methoxy analogue **13** was inactive (Table 1). These results are of interest as they indicate that in the Gram-negatives, **11–13** exhibit the same overall pattern of activity in cells as that observed for EcFPPS and PaFPPS enzyme inhibition (Table 1), for which **13** was inactive. Why there is less activity against *S. aureus* and *B. subtilis* is not known, and naturally could involve both differences in uptake/efflux as well as FPPS inhibition, although the latter possibility seems unlikely given the strong sequence similarities in the active site regions (Figure 3). Therefore, how can we further test whether FPPS is actually a target for **11** and **12** in the Gram-negative organisms?

To help answer this question, we first investigated whether there were synergistic effects between bisphosphonate **11** and fosmidomycin (**7**) in *E. coli*, *A. baumannii*, *K. pneumoniae*, and *P. aeruginosa*, basically as we described previously for **6** in *E. coli*. More specifically, we determined the fractional inhibitory concentration index (FICI) values for each combination using the FICI formula:^[14]

$$FICI = FIC_A + FIC_B = \frac{MIC(AB)}{MIC(A)} + \frac{MIC(BA)}{MIC(B)}$$

for which FIC_A and FIC_B are the fractional inhibitory concentrations of drugs A and B, $MIC(A)$ and $MIC(B)$ are the MIC values of drugs A and B acting alone, and $MIC(AB)$ and $MIC(BA)$ are the MIC values of the most effective combination of drug A or B in the presence of drug B or A. Using this method, FICI values of < 0.5 represent synergy, > 0.5 and < 1.0 represent additivity, > 1 and < 2 represent an indifferent effect, and ≥ 2 represents antagonism.^[15] In addition, we evaluated isobolograms using the method of Berenbaum.^[16] FICI values are shown in Table 2 and isobolograms in Figure 5. We found FICI values of 0.39 ± 0.15 (*E. coli*), 0.64 ± 0.23 (*A. baumannii*), 0.22 ± 0.026 (*K. pneumoniae*), and 0.44 ± 0.12 (*P. aeruginosa*); Table 2. FICI values of < 0.5 are generally taken to indicate a synergistic interaction, so these results are consistent with **11** inhibiting the same pathway as does fosmidomycin, that is, isoprenoid biosynthesis.

Another possible test to determine whether FPPS is a target is to see if cell growth inhibition can be “rescued” by the addition of farnesol. The use of farnesol, farnesyl diphosphate, geraniol, and geranylgeranyl diphosphate has been used previously—in mammalian cell lines as well as in trypanosomes (parasitic protozoa)—to assess the effects of bisphosphonates on cell growth, and in mammalian cell lines it is known that these kinases convert geranylgeraniol to geranylgeranyl diphosphate ($\text{GGOH} \rightarrow \text{GGPP}$),^[17] with GGOH rescuing cells from bisphosphonate growth inhibition. There are also kinases that can convert farnesol to farnesyl diphosphate ($\text{FOH} \rightarrow \text{FP}$), for example, but whether such prenyl kinases are present in the

Organism	MIC fos [$\mu\text{g mL}^{-1}$]	FIC fos	MIC 11 [$\mu\text{g mL}^{-1}$]	FIC 11	FICI ^[b]
<i>E. coli</i>	5	0.14 ± 0.13	6	0.24 ± 0.023	0.39 ± 0.15
<i>A. baumannii</i>	5	0.27 ± 0.057	6	0.37 ± 0.17	0.64 ± 0.23
<i>K. pneumoniae</i>	5	0.12 ± 0.014	6	0.097 ± 0.012	0.22 ± 0.026
<i>P. aeruginosa</i>	3	0.18 ± 0.066	10	0.27 ± 0.057	0.44 ± 0.12

[a] Data are the mean \pm SD for duplicate experiments. [b] Fractional inhibitory concentration index.

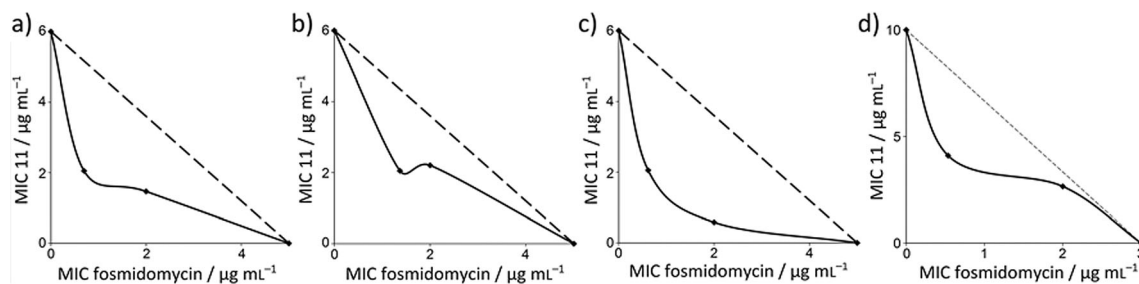


Figure 5. Isobolograms for bacterial cell growth inhibition by **11** and fosmidomycin (**7**) against a) *E. coli*, b) *A. baumannii*, c) *K. pneumoniae*, and d) *P. aeruginosa*. The fractional inhibitory concentration indices (FICI) are listed in Table 2. The mean FICI value is 0.42 ± 0.17 , indicating synergistic activity (in most cases).

organisms studied here is not known, so caution needs to be exercised in interpreting the results. We grew all four Gram-negative bacteria in the absence or presence of 200 μM FOH resulting in, on average, an approximate eightfold increase in IC_{50} for growth inhibition by the bisphosphonates **11** and **12**, consistent with an FPPS target (Figure 6).

Next, we carried out growth inhibition assays of **11** and **12** against an *E. coli* strain that overexpresses PaFPPS,^[18] again resulting in a considerable (~8-fold) increase in the IC_{50} values for both **11** and **12** (Table 3). Based on the patterns of FPPS and cell growth inhibition by **11**–**13**, synergistic activity with fosmidomycin, partial rescue of cell growth inhibition by FOH, and FPPS overexpression results, we conclude that the activity of **11** and **12** in Gram-negative bacteria is due—at least in part—to FPPS inhibition. The two active compounds **11** and **12** contain electron-withdrawing substituents and are likely to undergo charge-transfer interactions with the conserved Tyr79 (Figures 2 and 3), an interaction that would be absent with the methoxy side chain containing species **13**. It is also possible that there are additional targets, but the key point is that **11** and **12** are the first bisphosphonates to have promising (1–4 $\mu\text{g mL}^{-1}$) IC_{50} values against these four Gram-negative bacteria—values that are about an order of magnitude higher than found with **6**. FPPS is at least one of the targets involved, and there was little effect on HEK293 cell growth.

Alkyl phosphonate and carboxylate inhibitors

We next synthesized a series of hydroxy-substituted alkyl phosphonic acids and carboxylic acids. Our initial interest in these types of compound (structures shown in Figure S4) was that they might inhibit the enzyme dihydroxyacid dehydratase (DHAD), which in many bacteria is essential for branched-chain amino acid biosynthesis; for example, Flint and Nudelman reported the 2,3-dihydroxyoctanoic acid **14** (Figure 2) and the 1-hydroxy-2-methylpropylphosphonic acid **15** to be inhibitors of DHAD from plants and *E. coli*.^[19] The compounds were shown to bind enzymes that contain iron–sulfur clusters, but it appeared to us that they might also have prenyl transferase inhibitory activity. We therefore synthesized and tested a series of dihydroxy acids and hydroxyphosphonates (**16**–**41**, Figure S4) and tested them against the same panel of bacteria as described for the bisphosphonates: *S. aureus*, *B. subtilis*,

Table 3. IC_{50} values of compounds **11**, **12**, **32**, and **41** in *E. coli*, *A. baumannii*, *K. pneumoniae*, *P. aeruginosa*, *E. coli* overexpressing *P. aeruginosa* FPPS (PaFPPS⁺⁺), and *E. coli* overexpressing *E. coli* UPPS (EcUPPS⁺⁺).

Organism	Inhibitor	Rescuing Agent (RA)	IC_{50} [$\mu\text{g mL}^{-1}$] ^[a]	
			without RA	with RA
<i>E. coli</i>	11	Farnesol	2.1 \pm 0.57	19 \pm 4.1
<i>E. coli</i>	12	Farnesol	1.7 \pm 0.38	28 \pm 9.0
<i>A. baumannii</i>	11	Farnesol	2.8 \pm 0.70	18 \pm 4.9
<i>A. baumannii</i>	12	Farnesol	2.0 \pm 0.50	22 \pm 2.4
<i>K. pneumoniae</i>	11	Farnesol	2.3 \pm 0.49	13 \pm 1.8
<i>K. pneumoniae</i>	12	Farnesol	2.4 \pm 0.43	21 \pm 4.2
<i>P. aeruginosa</i>	11	Farnesol	3.5 \pm 0.78	23 \pm 7.8
<i>P. aeruginosa</i>	12	Farnesol	3.3 \pm 0.68	22 \pm 3.5
<i>E. coli</i>	11	PaFPPS ⁺⁺	1.6 \pm 0.35	19 \pm 2.4
<i>E. coli</i>	12	PaFPPS ⁺⁺	2.5 \pm 1.1	15 \pm 3.6
<i>E. coli</i>	32	EcUPPS ⁺⁺	6.4 \pm 1.3	86 \pm 17
<i>E. coli</i>	41	EcUPPS ⁺⁺	9.0 \pm 1.5	107 \pm 15

[a] Data are the mean \pm SD for duplicate experiments.

M. smegmatis, *E. coli*, *A. baumannii*, *K. pneumoniae*, and *P. aeruginosa*. Compounds **16**, **17**, **23**, **24**, **26**, **28**, **29**, and **34**–**38** were found to be inactive. Results for all active compounds are shown in Table S1 (SMILES structures in Table S2) and Figure S5, and results for the most active compounds are listed in Table 4. Several compounds containing long alkyl side chains, such as **32** and **41**, had activity in the 2–6 $\mu\text{g mL}^{-1}$ range against Gram-positive, but not Gram-negative bacteria (Table 4). These results then raise the question: how do these compounds inhibit bacterial cell growth?

We reasoned that isoprenoid biosynthesis might again be one target area since there is some similarity between the more potent bacterial cell growth inhibitors—the lipophilic hydroxyphosphonates **32** and **41**—and GPP or FPP, substrates involved in many prenyl transferase reactions. To determine whether isoprenoid biosynthesis inhibition was a likely target, we carried out 12 FICI determinations using the 1-hydroxyphosphonate **32** together with either a known antibacterial isoprenoid/cell wall biosynthesis inhibitor (fosmidomycin, carbenicillin, vancomycin, ampicillin, bacitracin, cefotaxime, fosfomycin) or an antibacterial compound that does not target these pathways (kanamycin, tetracycline, chloramphenicol, spectinomycin, sulfamethoxazole, trimethoprim). We obtained

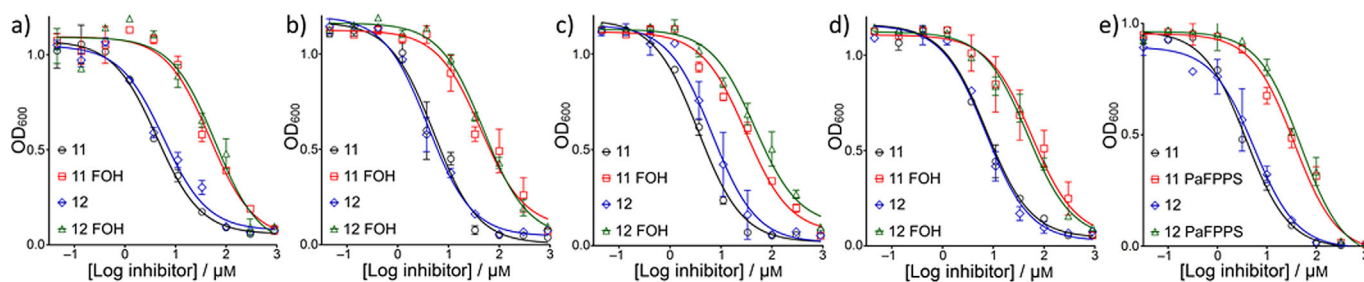
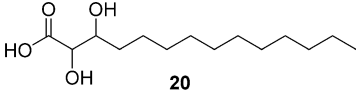
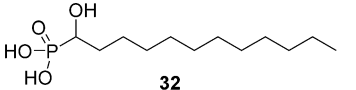
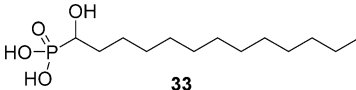
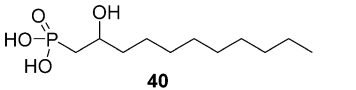
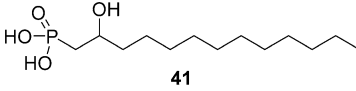


Figure 6. Partial rescue of cell growth inhibition by farnesol or PaFPPS overexpression. Addition of 200 μM farnesol (FOH) to the growth medium increases the IC_{50} values of **11** and **12** for cell growth inhibition by a factor of ~8. a) *E. coli* K-12 with FOH; b) *A. baumannii* with FOH; c) *K. pneumoniae* with FOH; d) *P. aeruginosa* with FOH; and e) *E. coli* BL21(DE3) with PaFPPS overexpression.

Table 4. IC₅₀ values of dihydroxy acids and hydroxyphosphonates against bacterial cells and enzymes.

Compound	IC ₅₀ [μg mL ⁻¹]							IC ₅₀ [μM]	
	<i>S. aureus</i>	<i>B. subtilis</i>	<i>M. smegmatis</i>	<i>E. coli</i>	<i>A. baumannii</i>	<i>K. pneumoniae</i>	<i>P. aeruginosa</i>	SaUPPS	EcUPPP
 20	5.2	39	14	8.1	> 100	> 100	> 100	39	> 200
 32	1.7	2.0	3.7	6.4	5.9	6.4	37	0.73	0.92
 33	3.1	5.0	8.7	8.1	6.2	24	> 100	2.4	3.7
 40	> 100	> 100	21	> 100	> 100	> 100	> 100	25	11
 41	6.4	10	7.0	9.0	14	25	> 100	2.8	3.4

data on two organisms: *B. subtilis*, chosen because it uses the non-mevalonate (MEP) pathway and is inhibited by fosmidomycin (which targets 1-deoxy-D-xylulose 5-phosphate reductoisomerase, DXR), and *S. aureus*, which uses the mevalonate pathway.

Typical experimental (isobologram) results are shown in Figure 7 and Figure S6, and the FICI results are listed in Table 5. The results indicate that for each case in which the second inhibitor targets isoprenoid/cell wall biosynthesis, there is a synergistic interaction (FICI_{avg} = 0.31 ± 0.11, *n* = 13), whereas for cases in which the second inhibitor is not involved in isoprenoid/cell wall biosynthesis, there is an indifferent (albeit not antagonistic) effect (FICI_{avg} = 1.53 ± 0.19, *n* = 11). We again use the definition that FICI values < 0.5 mean synergy, 0.5–1 additivity, 1–2 indifference, and > 2 antagonism. These results strongly support the idea that this hydroxyphosphonate, **32**, targets isoprenoid/cell wall biosynthesis. Some possible tar-

gets, based on structure, would be FPPS, UPPS, and UPPP, as these are all in the isoprenoid/cell wall biosynthesis pathway (where we see synergy) while for example, prenyl synthases, such as those involved in quinone biosynthesis, are not.

We then tested all compounds against EcFPPS, SaUPPS, and EcUPPP^[20] using phosphate-release assays.^[21] There was no activity (IC₅₀ > 300 μM) against EcFPPS or PaFPPS (data not shown), but several compounds (Figures S7 and S8) were found to be active against UPPS and UPPP, and dose–response curves for the most active species are shown in Figure 8a,b. Both the 1-OH and 2-OH phosphonates (**32** and **41**) were active against SaUPPS, with IC₅₀ values of ~1–3 μM. For the UPPP activity inhibition assay, we found that **32** and **41** inhibited UPPP with IC₅₀ values of ~1–4 μM (corresponding to K_i ~ 300–980 nM, assuming competitive inhibition).^[22] Under the same assay conditions, the IC₅₀ value for UPPP inhibition by bacitracin was 32 μM (Figure 8b). So, compounds **32** and **41** in-

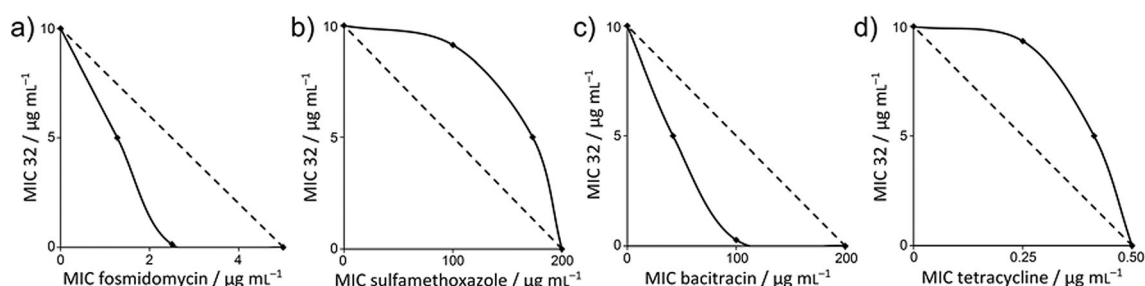
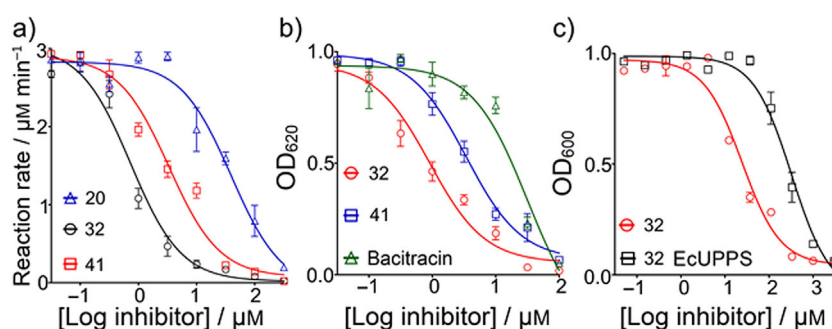


Figure 7. Representative isobolograms for **32** with antibiotics having known mechanisms of action. a) **32** + fosmidomycin in *B. subtilis* showing synergy (FICI = 0.27) of **32** with a cell wall biosynthesis inhibitor (that targets 1-deoxy-D-xylulose-5-phosphate reductoisomerase (DXR) in the non-mevalonate pathway); b) **32** + sulfamethoxazole in *B. subtilis* showing an indifferent effect (FICI = 1.78) of **32** with a nucleic acid biosynthesis inhibitor (that targets dihydropterotate synthase); c) **32** + bacitracin in *S. aureus* showing synergy (FICI = 0.24) of **32** with a cell wall biosynthesis inhibitor (that targets UPPP); d) **32** + tetracycline in *S. aureus* showing an indifferent effect (FICI = 1.61) of **32** with a protein synthesis inhibitor (that targets ribosome function).

Table 5. Effects of the addition of various known bacterial cell growth inhibitors on the inhibition of *B. subtilis* and *S. aureus* cell growth by compound **32**. The cell targets of the known inhibitors are listed, together with the FICI values (and errors) for the combinations.^[a]

	Antibiotic	MIC antibiotic [$\mu\text{g mL}^{-1}$]	FIC antibiotic	MIC 32 [$\mu\text{g mL}^{-1}$]	FIC 32	FICI
<i>B. subtilis</i>						
Cell Wall Biosynthesis Inhibitors	fosmidomycin	5	0.25 ± 0.043	10	0.013 ± 0.0037	0.27 ± 0.046
	carbenicillin	5	0.25 ± 0.043	10	0.097 ± 0.049	0.34 ± 0.048
	cefotaxime	2.5	0.30 ± 0.044	10	0.075 ± 0.012	0.38 ± 0.056
	vancomycin	0.5	0.33 ± 0.058	10	0.080 ± 0.059	0.41 ± 0.12
	fosfomycin	200	0.21 ± 0.025	10	0.22 ± 0.052	0.43 ± 0.077
	ampicillin	0.5	0.18 ± 0.041	10	0.048 ± 0.023	0.23 ± 0.063
	bacitracin	200	0.12 ± 0.028	10	0.23 ± 0.010	0.35 ± 0.13
Protein Biosynthesis Inhibitors	kanamycin	1.5	0.61 ± 0.097	10	0.95 ± 0.097	1.55 ± 0.19
	tetracycline	5	0.82 ± 0.21	10	0.80 ± 0.15	1.61 ± 0.35
	chloramphenicol	0.5	0.55 ± 0.13	10	0.93 ± 0.32	1.47 ± 0.45
Nucleic Acid Inhibitors	sulfamethoxazole	200	0.87 ± 0.23	10	0.91 ± 0.25	1.78 ± 0.48
	trimethoprim	0.5	0.77 ± 0.18	10	0.60 ± 0.084	1.37 ± 0.26
<i>S. aureus</i>						
Cell Wall Biosynthesis Inhibitors	carbenicillin	15	0.27 ± 0.015	10	0.052 ± 0.0077	0.32 ± 0.022
	cefotaxime	2	0.21 ± 0.048	10	0.18 ± 0.057	0.40 ± 0.11
	vancomycin	1.5	0.19 ± 0.019	10	0.16 ± 0.033	0.34 ± 0.052
	fosfomycin	200	0.13 ± 0.022	10	0.052 ± 0.014	0.18 ± 0.036
	ampicillin	0.5	0.30 ± 0.095	10	0.056 ± 0.012	0.35 ± 0.11
	bacitracin	200	0.21 ± 0.039	10	0.027 ± 0.0090	0.24 ± 0.048
Protein Biosynthesis Inhibitors	kanamycin	1.5	0.81 ± 0.17	10	0.83 ± 0.17	1.64 ± 0.34
	tetracycline	0.5	0.83 ± 0.38	10	0.93 ± 0.13	1.76 ± 0.51
	chloramphenicol	5	0.71 ± 0.11	10	0.73 ± 0.21	1.44 ± 0.33
	spectinomycin	40	0.45 ± 0.091	10	0.84 ± 0.22	1.29 ± 0.31
Nucleic Acid Inhibitors	sulfamethoxazole	200	0.75 ± 0.20	10	0.99 ± 0.17	1.74 ± 0.37
	trimethoprim	15	0.69 ± 0.32	10	0.53 ± 0.13	1.22 ± 0.45
Mean FICIs:	<i>B. subtilis</i>	inhibitors targeting cell wall biosynthesis				0.31 ± 0.14
		inhibitors targeting nucleic acids and protein biosynthesis				1.56 ± 0.15
	<i>S. aureus</i>	inhibitors targeting cell wall biosynthesis				0.31 ± 0.080
		inhibitors targeting nucleic acids and protein biosynthesis				1.52 ± 0.23

[a] The mean value for isoprenoid/cell wall biosynthesis inhibitors is $\text{FICI}_{\text{avg}} = 0.31 \pm 0.11$, $n = 13$ (indicating synergistic activity); that for other inhibitors is $\text{FICI}_{\text{avg}} = 1.53 \pm 0.19$, $n = 11$ (indicating an indifferent although not antagonistic effect). Data are the mean \pm SD for duplicate experiments.

**Figure 8.** Enzyme and cell growth inhibition by the dihydroxyacid **20** and hydroxyphosphonates **32** and **41**. a) SaUPPS inhibition; b) EcUPPP inhibition together with result for bacitracin; c) partial rescue of *E. coli* cell growth inhibition by EcUPPS overexpression.

hibit both UPPS as well as UPPP, consistent with the observation that **32** shows synergistic activity with all isoprenoid/cell wall biosynthesis inhibitors tested. The dihydroxy acid **20** showed weak inhibition against SaUPPS and no inhibition ($> 200 \mu\text{M}$) against EcUPPP, resulting in less activity in cells. We

also found that overexpressing EcUPPS caused an approximate sixfold increase in the IC_{50} value for *E. coli* cell growth inhibition by both **32** and **41** (Figure 7c and Figure S9). We therefore conclude that both UPPS as well as UPPP are likely targets for the most potent hydroxyphosphonates. Because **32** and **11** in-

hibit different enzymes involved in isoprenoid biosynthesis, we also tested for synergistic activity against *E. coli* cell growth. As expected, **32** and **11** have synergistic activity with an FICI value of 0.31 ± 0.099 (Figure S10). Finally, we tested **20**, **32**, and **41** for their effects on growth of the human embryonic kidney cell line HEK293. The MIC values for cell growth inhibition were in the range of $90\text{--}410 \mu\text{g mL}^{-1}$ (Figure S3), so these compounds are not highly toxic toward at least this human cell line.

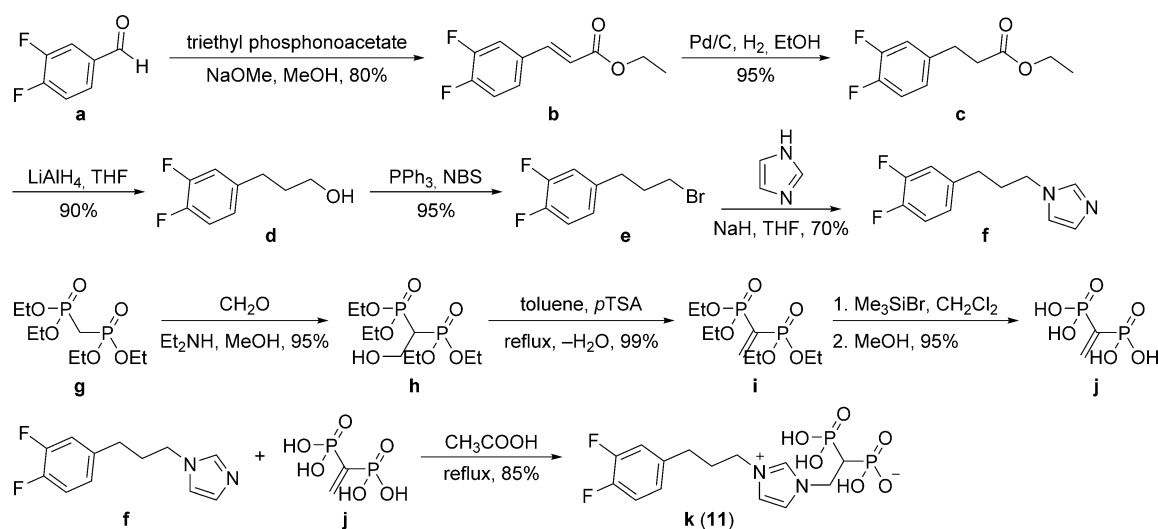
Conclusions

The results we report herein are of interest for several reasons. We synthesized a broad range of compounds—bisphosphonates, hydroxyphosphonates, and dihydroxyacids—to identify novel inhibitors of isoprenoid biosynthesis that also inhibit bacterial cell growth. Based on earlier work on *E. coli* cell growth inhibition and the structure of a *T. brucei* FPPS–bisphosphonate complex, we made novel bisphosphonates containing electron-withdrawing aryl substituents that inhibited *E. coli*, *K. pneumoniae*, *A. baumannii*, and *P. aeruginosa* cell growth in the $1\text{--}4 \mu\text{g mL}^{-1}$ range. Growth inhibition was partially rescued (an increase in IC_{50} by a factor of ~ 8) by the addition of farnesol, and in cells overexpressing FPPS, FICI values for one bisphosphonate with fosmidomycin were 0.42 ± 0.17 , consistent with an isoprenoid biosynthesis target. We also produced a series of dihydroxy acids and hydroxyphosphonates which we found to inhibit UPPS as well as UPPP, along with Gram-positive (but not Gram-negative) bacterial cell growth. These compounds, as well as the bisphosphonates, acted synergistically with other known inhibitors of isoprenoid biosynthesis/bacterial cell wall growth. Overall, the results are of interest because we have found several new prenyl synthase inhibitors that target FPPS, UPPS, or UPPP, that also have low micromolar activity against numerous pathogenic bacteria.

Experimental Section

General methods: All chemicals were reagent grade. ^1H and ^{13}C NMR spectra were obtained on Varian Unity spectrometers (Palo Alto, CA, USA) at 400 and 500 MHz for ^1H and at 100 and 125 MHz for ^{13}C . Elemental analyses were carried out in the University of Illinois Microanalysis Laboratory. HPLC–MS analyses were performed with an Agilent LC–MSD Trap XCT Plus system (Agilent Technologies, Santa Clara, CA, USA) with an 1100 series HPLC system including a degasser, an autosampler, a binary pump, and a multiple wavelength detector. All final compounds were $\geq 95\%$ pure as determined by quantitative spin count NMR (qNMR) or HPLC–MS, and structures were characterized by ^1H NMR and HRMS.

Chemical syntheses: Hydrogen (2-(3-(3-(3,4-difluorophenyl)propyl)-1H-imidazol-3-ium-1-yl)-1-phosphonoethyl) phosphonate (11). To a solution of 3,4-difluorobenzaldehyde **a** (1.4 g, 10 mmol) in 20 mL methanol was added triethyl phosphonoacetate (3 mL, 15 mmol; Scheme 1). The reaction mixture was cooled to 0°C and into it was slowly added 2 mL sodium methoxide (30 wt% solution in methanol). The mixture was stirred overnight at room temperature. The solvent was removed under reduced pressure, and the crude material partitioned between ethyl acetate and water. The organic layer was dried over Na_2SO_4 , and solvent removed under reduced pressure. The product was purified by column chromatography (silica gel, eluting with hexane/ethyl acetate 30:1) to give the unsaturated ester **b** as an oil (1.7 g, 80%). To a solution of **b** (1.7 g, 8 mmol) in methanol (100 mL) was added palladium on charcoal (0.6 g, 10%) under hydrogen. The reaction mixture was stirred at room temperature for 3 h. Solvents were removed under reduced pressure. The product was partitioned between water and ethyl acetate, the organic layer separated, dried over Na_2SO_4 , and solvent removed under reduced pressure. The ester product **c** was obtained as a colorless oil (1.6 g, 95%). To a solution of lithium aluminum hydride (160 mg, 4 mmol) in anhydrous tetrahydrofuran (THF) was slowly added a solution of **c** (1.6 g, 8 mmol) in THF (30 mL). The reaction mixture was stirred at room temperature overnight. Then, water (12 mL), sodium hydroxide (4 N, 12 mL) and finally water (36 mL) were added at 0°C . The mixture was stirred, and the resulting salts filtered through a pad of Celite, washing with ethyl acetate (100 mL). The product was treated with water



Scheme 1. Synthesis route to FPPS inhibitors 11–13.

and CH_2Cl_2 and the organic layer separated, dried over Na_2SO_4 , and solvent removed under reduced pressure to give the alcohol product **d** as an oil (1.0 g, 90%). To a solution of **d** (1.0 g, 7 mmol) in 100 mL CH_2Cl_2 was added triphenylphosphine (2.3 g, 8 mmol). The mixture was stirred at room temperature, and *N*-bromosuccinimide (NBS, 1.4 g, 8 mmol) added in small portions. The mixture was stirred overnight then washed with water and extracted with hexane. The organic layer was separated, dried over Na_2SO_4 , and solvent removed under reduced pressure to give the bromide product **e** as a light-yellow solid (1.5 g, 95%). Imidazole (1.0 g, 15 mmol) was dissolved in THF (30 mL), and NaH (240 mg, 10 mmol) was added. The mixture was stirred at room temperature for 30 min, then **e** (1.5 g, 7 mmol) was added. The reaction mixture was heated at 80°C and stirred overnight, then quenched with water, and the mixture was extracted with diethyl ether. The organic layer was separated, dried over Na_2SO_4 , and solvent removed under reduced pressure. The crude product was purified by column chromatography (silica gel, hexane/ethyl acetate 2:1). The imidazole product **f** was obtained as a light-yellow solid (1.05 g, 70%). Paraformaldehyde (1.35 g, 45.0 mmol) and diethylamine (0.68 g, 9.33 mmol) were dissolved in dry methanol (30 mL), with warming. A solution of tetraethyl methylenebisphosphonate **g** (2.7 g, 9.33 mmol) in dry methanol (30 mL) was added at 20°C , and the mixture stirred for five days. The reaction mixture was then concentrated under vacuum, toluene (20 mL) was added, and the solution was concentrated again. This last step was then repeated to remove all traces of methanol, yielding tetraethyl 1-methoxymethyl methylene 1,1-bisphosphonate **h** as a colorless oil (2.9 g, 95%). Intermediate **h** was added to *p*TSA (cat) and toluene (100 mL), and the mixture was heated for 16 h at reflux with a Soxhlet apparatus charged with 4 Å molecular sieves. The mixture was allowed to cool to 20°C , then washed with water (2×20 mL). Drying (MgSO_4) and concentrating under vacuum gave **i** as a colorless viscous oil (2.7 g, 99%). Intermediate **i** (2.7 g, 9 mmol) was dissolved in dry CH_2Cl_2 , cooled to 0°C , and Me_3SiBr (12 mL, 90 mmol) was added dropwise over 30 min. The mixture was stirred for two days at room temperature. The solvent was then evaporated, and the residue was dried under vacuum for ~ 1 h. Then, 80 mL dry methanol was added, and the mixture was stirred for 20 min at room temperature. The solvent was removed, and the brown oil was dried overnight to give compound **j** (1.6 g, 95%). Intermediate **f** (220 mg, 1 mmol) was dissolved in AcOH, then **j** (206 mg, 1.1 mmol) was slowly added. The mixture was stirred at reflux for three days. The AcOH was then evaporated under vacuum. The residue was suspended in methanol and sonicated for 1 min. The mixture was then centrifuged, and the liquid layer discarded. The latter procedure was repeated twice. Then, the remaining residue was dried under vacuum overnight to give the final product **k** (**11**) as a white solid (3.1 g, 85%). $^1\text{H NMR}$ (D_2O ,

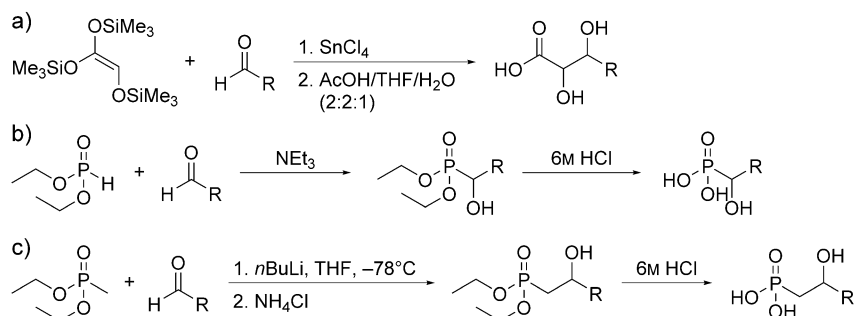
500 MHz): $\delta = 8.62$ (s, 1 H), 7.39 (s, 1 H), 7.24 (s, 1 H), 7.00 (m, 2 H), 6.80 (m, 1 H), 4.43 (dt, $J = 7.0, 12.5$ Hz, 2 H), 4.02 (t, $J = 7.5$ Hz, 2 H), 2.50 (t, $J = 7.5$ Hz, 2 H), 2.41 (tt, $J = 7.0, 12.5$ Hz, 1 H), 2.04 ppm (m, 2 H); $^{31}\text{P NMR}$ (D_2O , 202 MHz): $\delta = 15.29$ ppm; ESI HRMS: m/z [$M + \text{H}$] $^+$ calcd for $\text{C}_{14}\text{H}_{19}\text{F}_2\text{N}_2\text{O}_6\text{P}_2^+$: 411.0686, found: 411.0690. The purity of the product was determined by qNMR (potassium hydrogen phthalate as standard, 99.95%): 98.3%.

General procedure for 2,3-dihydroxy acids: 2,3-Dihydroxy acids were synthesized according to a published method (Scheme 2a).^[23] To a stirred mixture of the corresponding aldehyde (10 mmol) and tris(trimethylsilyloxy) ethylene (2.9 g, 10 mmol), 1–2 drops of tin(IV) chloride were added (*exothermic*). After stirring for 3 h, 2:2:1 acetic acid/THF/water (20 mL) was added. The solutions were stirred for 10 min, and solvents were removed under reduced pressure at 50 – 60°C . Toluene was added and removed, twice. The residues were recrystallized from chloroform/methanol to give the 2,3-dihydroxy acids.

General procedure for (1-hydroxy)phosphonic acids: 1-Hydroxyphosphonic acids were synthesized according to a published method (Scheme 2b).^[24] To a stirred solution of diethyl phosphite (1.4 g, 10 mmol) and triethylamine (1.0 g, 10 mmol), the corresponding aldehyde (10 mmol) was added dropwise, at room temperature (*exothermic*). After addition was complete, the reaction mixture was kept at room temperature overnight. The mixtures were concentrated, and the residues were purified by column chromatography on silica (hexane/ethyl acetate) to give the 1-hydroxyalkyl phosphonates, which were then treated with 6 M hydrochloric acid (20 equiv). The resulting solutions were held at reflux under N_2 for 1–2 days. The reaction mixtures were then concentrated and subjected to high vacuum, yielding the 1-hydroxyphosphonic acids.

General procedure for (2-hydroxy)phosphonic acids: To a solution of diethyl methylphosphonate (152 mg, 1 mmol) in THF (5 mL) was added 1.2 equiv 1.6 M *n*BuLi at -78°C , Scheme 2c. The solution was stirred at the same temperature for 1 h. A solution of corresponding aldehyde (1 mmol) in THF (5 mL) was slowly added. The resulting solution was stirred for 30 min at -78°C and then quenched by the addition of saturated aqueous NH_4Cl . The aqueous phase was extracted with Et_2O . The combined organic layers were concentrated and the product purified by column chromatography on silica (hexane/ethyl acetate) to give the 2-hydroxyalkyl phosphonate, which was then treated with 6 M hydrochloric acid (20 equiv). The resulting solution was held at reflux under N_2 for 1–2 days, concentrated, then subjected to high vacuum, yielding the 2-hydroxyphosphonic acids.

E. coli growth inhibition assay: IC_{50} values for *E. coli* cell growth inhibition were determined using a microdilution method. Station-



Scheme 2. General methods for synthesis of: a) 2,3-dihydroxy acids; b) 1-hydroxyphosphonic acids; c) 2-hydroxyphosphonic acids.

ary overnight starter cultures of *E. coli* (K-12 or BL21(DE3) strains), were diluted 1000-fold and grown to an OD₆₀₀ value of ~0.3. These log-phase cultures were then diluted 500-fold into fresh LB broth to generate a working solution; 200 µL of working solution was transferred into each well of a 96-well culture plate (Corning 3370). Inhibitors were then added at 1 mM and sequentially diluted threefold to 46 nM, keeping volume and culture broth composition constant. Plates were incubated for 12 h at 37 °C, shaking at 200 rpm. Absorbance at 600 nm was then measured to assess bacterial cell growth. IC₅₀ values were determined using nonlinear regression, whereas minimum inhibitory concentration (MIC) values in the synergy assays were calculated by using a Gompertz function in Prism 5 (GraphPad Software Inc., La Jolla, CA, USA).

Gram-negative bacterial cell growth inhibition assay: As with the *E. coli* inhibition assays, overnight cultures (in cation-adjusted Mueller–Hinton broth, CAMHB) of *A. baumannii* (Bouvet and Grimont, ATCC 19606); *K. pneumoniae* (subsp. *pneumoniae* Schroeter Trevisan ATCC 27736); and *P. aeruginosa* (PA01) were diluted 1000-fold (in fresh CAMHB) to create a working solution. Working solutions were then transferred into flat-bottom 96-well plates, and inhibitors added at 1 mM and sequentially diluted threefold to 46 nM. Plates were incubated at 37 °C, shaking at 200 rpm, overnight. The OD₆₀₀ value was then measured to determine bacterial growth inhibition.

***B. subtilis* growth inhibition assay:** An overnight starter culture (in LB broth) of *B. subtilis* (subsp. *subtilis* (Ehrenberg) Cohn ATCC 6051) was diluted 1000-fold (in fresh LB media) to create a working solution. Working solutions were then transferred into flat-bottom 96-well plates, and inhibitors were added at 1 mM and sequentially diluted threefold to 46 nM. Plates were incubated at 37 °C, shaking at 200 rpm overnight. The OD₆₀₀ value was then measured to determine bacterial growth inhibition.

***S. aureus* growth inhibition assay:** An overnight starter culture of *S. aureus* (Newman strain) in tryptic soy broth was diluted 1000-fold in fresh tryptic soy media to create a working solution. Working solutions were transferred into flat-bottom 96-well plates and inhibitors added at 1 mM and sequentially diluted threefold to 46 nM. Plates were incubated at 37 °C, shaking at 200 rpm overnight. The OD₆₀₀ value was then measured to determine bacterial growth inhibition.

HEK293 toxicity assay: A frozen stock of human embryonic kidney cells (HEK293 ATCC CRL-1573) was used to grow a first generation of cells in DMEM (4.5 g L⁻¹ glucose with L-glutamine) containing 10% fetal bovine serum (FBS) and 1% penicillin–streptomycin (10000 U mL⁻¹). This generation was harvested in 0.25% trypsin/2.1 µM EDTA, and cells were counted under a light microscope. A working solution was generated containing 10⁵ cells per mL, which was then transferred into a flat-bottom 96-well plate for 36 h. At this time, 20 µL of inhibitor solutions ranging from 1 mM to 46 nM were added, and cells were allowed to grow in the presence of the inhibitors for an additional 24 h. MTT solution (10 µL, 5 mg mL⁻¹ in PBS) was then added to each well and incubated for 4 h. HCl in isopropanol (100 µL of 100 mM) was added to each well, and absorbance at 570 nm was measured. MIC values were calculated by using a Gompertz function in Prism 5 (GraphPad Software Inc., La Jolla, CA, USA).

Synergy/antagonism assays: To investigate possible synergistic interactions between compound **11** and fosmidomycin as well as compound **32** and a range of antibiotics, we carried out two-drug combination assays. Bacteria were incubated with a threefold gradient of antibiotic typically ranging from 40 µg mL⁻¹ to 18 ng mL⁻¹

(200 µg mL⁻¹ to 90 ng mL⁻¹ for bacitracin, fosfomycin, and sulfamethoxazole) in the presence half-MIC concentrations of **11** and **32**, in addition to a threefold gradient of **11** and **32** ranging from 40 µg mL⁻¹ to 18 ng mL⁻¹ in the presence of half-MIC concentrations of each antibiotic. New MIC values were calculated by using a Gompertz function in Prism 5 (GraphPad Software Inc., La Jolla, CA, USA).

Enzyme inhibition assays: FPPS, SaUPPS, and EcUPPP were expressed and purified as described previously.^[3,5,9,10,12,19,22] FPPS and UPPS assays were carried out using a phosphate release assay.^[5,21] Depending on the solubility, bisphosphonates, hydroxyphosphonates, and dihydroxy acid inhibitors were prepared as 10 mM stock solutions in DMSO or basic water (pH ~10) and then serially diluted from 1 mM to 1 nM. Inhibitors were incubated with 25 ng SaUPPS at room temperature for 10 min in a pH 7.5 buffer (50 mM HEPES, 150 mM NaCl, 10 mM MgCl₂, and 0.02% *n*-dodecyl-β-D-maltopyranoside) before adding a reaction mixture containing 5 µM FPP, 50 µM IPP, 3 U mL⁻¹ purine nucleoside phosphorylase, 1 U mL⁻¹ inorganic phosphatase, and ~600 µM 7-methyl-6-thioguanosine (MESG), again in the same buffer. For FPPS inhibition assay, inhibitors were incubated with 25 ng of various FPPS enzymes at room temperature for 10 min in a pH 7.0 buffer (10 mM HEPES, 150 mM NaCl, 5 mM MgCl₂) before adding a reaction mixture containing 50 µM GPP, 50 µM IPP, 3 U mL⁻¹ purine nucleoside phosphorylase, 1 U mL⁻¹ inorganic phosphatase, and ~600 µM 7-methyl-6-thioguanosine (MESG), again in the same buffer. FPPS and UPPS reactions were monitored for 15 min with the rate of increase in absorbance at 360 nm taken as the rate of FPP or UPP synthesis, respectively. IC₅₀ values were calculated by using Prism 5 (GraphPad Software Inc., La Jolla, CA, USA). The UPPP inhibition assay was carried out using a malachite-green reagent as described previously.^[25] The same 10 mM inhibitor stock solutions and assay buffer as for the SaUPPS assays were used to test for UPPP inhibition. Inhibitors were incubated with 20 nM EcUPPP at room temperature for 15 min before adding FPP to 35 µM. Reaction mixtures were incubated at 37 °C for 20 min, then quenched by adding 30 µL malachite-green reagent. In this assay, the phosphate released from FPP reacts with ammonium molybdate to form phosphomolybdate (yellow), which then forms a complex (λ_{max} ~620 nm) with malachite-green, used to assess phosphatase activity. Phosphate release was measured at 620 nm and quantified based on a phosphate standard curve, and the OD₆₂₀ values used to construct dose–response curves.

Supporting Information: Enzyme and cell growth inhibition tables and graphs, isobolograms, compound synthesis and characterization, HPLC purity results, ¹H NMR spectra of inhibitor compounds.

Acknowledgements

This work was supported by the United States Public Health Service (NIH grants CA158191 and GM065307), a Harriet A. Harlin Professorship, and the University of Illinois Foundation/Oldfield Research Fund. The authors thank Dr. Robert Schnell and Professor Gunter Schneider for providing the *P. aeruginosa* FPPS expression system and Professor Douglas Mitchell for providing the bacteria.

Keywords: cell wall biosynthesis · drug discovery · Gram-negative pathogens · membrane proteins · *Staphylococcus aureus*

- [1] *Antibiotic Resistance Threats in the United States, 2013*, US Department of Health and Human Services, Centers for Disease Control and Prevention (CDC): <http://www.cdc.gov/drugresistance/pdf/ar-threats-2013-508.pdf>.
- [2] a) E. Oldfield, X. Feng, *Trends Pharmacol. Sci.* **2014**, *35*, 664–674; b) E. D. Brown, G. D. Wright, *Nature* **2016**, *529*, 336–343.
- [3] A. Leon, L. Liu, Y. Yang, M. P. Hudock, P. Hall, F. Yin, D. Studer, K. J. Puan, C. T. Morita, E. Oldfield, *J. Med. Chem.* **2006**, *49*, 7331–7341.
- [4] H. Jomaa, J. Wiesner, S. Sanderbrand, B. Altincicek, C. Weidemeyer, M. Hintz, I. Turbachova, M. Eberl, J. Zeidler, H. K. Lichtenthaler, D. Soldati, E. Beck, *Science* **1999**, *285*, 1573–1576.
- [5] W. Zhu, Y. Zhang, W. Sinko, M. E. Hensler, J. Olson, K. J. Molohon, S. Lindert, R. Cao, K. Li, K. Wang, *Proc. Natl. Acad. Sci. USA* **2013**, *110*, 123–128.
- [6] M. A. Farha, T. L. Czarny, C. L. Myers, L. J. Worrall, S. French, D. G. Conrady, Y. Wang, E. Oldfield, N. C. Strynadka, E. D. Brown, *Proc. Natl. Acad. Sci. USA* **2015**, *112*, 11048–11053.
- [7] X. Feng, W. Zhu, L. A. Shurig-Briccio, S. Linder, C. Shoen, R. Hitchings, J. Li, Y. Wang, N. Baig, T. Zhou, B. K. Kim, D. C. Cric, *Proc. Natl. Acad. Sci. USA* **2015**, *112*, E7073–E7082.
- [8] L. Widler, K. A. Jaeggi, M. Glatt, K. Muller, R. Bachmann, M. Bisping, A.-R. Born, R. Cortesi, G. Guiglia, H. Jeker, et al., *J. Med. Chem.* **2002**, *45*, 3721–3738.
- [9] R. Cao, C. K. Chen, R. T. Guo, A. H. Wang, E. Oldfield, *Proteins Struct. Funct. Bioinf.* **2008**, *73*, 431–439.
- [10] P. D. Ziniel, J. Desai, C. L. Cass, C. Gatto, E. Oldfield, D. L. Williams, *Antimicrob. Agents Chemother.* **2013**, *57*, 5969–5976.
- [11] Y. Song, J. M. Chan, Z. Tovian, A. Secrest, E. Nagy, K. Krysiak, K. Bergan, M. A. Parniak, E. Oldfield, *Bioorg. Med. Chem.* **2008**, *16*, 8959–8967.
- [12] Y. Xia, Y. L. Liu, Y. Zie, W. Zhu, F. Guerra, S. Shen, N. Yeddule, W. Fischer, W. Low, X. Zhou, Y. Zhang, E. Oldfield, I. M. Verma, *Sci. Transl. Med.* **2014**, *6*, 263ra161.
- [13] S. Mukherjee, C. Huang, F. Guerra, K. Wang, E. Oldfield, *J. Am. Chem. Soc.* **2009**, *131*, 8374–8375.
- [14] a) G. M. Eliopoulos, R. C. Moellering in *Antibiotics in Laboratory Medicine* (Ed.: V. Lorian), Williams & Wilkins Publishing Co., **1998**, pp. 330–396; b) P. K. Singh, B. F. Tack, P. B. McCray, M. J. Welsh, *Am. J. Physiol. Lung Cell Mol. Physiol.* **2000**, *279*, L799–805.
- [15] European Committee for Antimicrobial Susceptibility Testing (EUCAST) of the European Society of Clinical Microbiology and Infectious Diseases (ESCMID), *Clin. Microbiol. Infect.* **2000**, *6*, 503–508.
- [16] M. C. Berenbaum, *Pharmacol. Rev.* **1989**, *41*, 93–141.
- [17] a) J. E. Fisher, M. J. Rogers, J. M. Halasy, S. P. Luckman, D. E. Hughes, P. J. Masracha, G. Wesolowski, R. G. Russell, G. A. Rodan, A. A. Reszka, *Proc. Natl. Acad. Sci. USA* **1999**, *96*, 133–138; b) E. van Beek, C. Löwik, G. van der Pluijm, S. Papapoulos, *J. Bone Miner. Res.* **1999**, *14*, 722–729.
- [18] J. W. Schmidberger, R. Schnell, G. Schneider, *Acta. Crystallogr. Sect. D* **2015**, *71*, 721–731.
- [19] D. H. Flint, A. Nudelman, *Bioorg. Chem.* **1993**, *21*, 367–385.
- [20] M. F. Hsu, T. F. Yu, C. C. Chou, H. Y. Fu, C. S. Yang, A. H. Wang, *PLoS One* **2013**, *8*, e56363.
- [21] a) M. D. Hartley, A. Larkin, B. Imperiali, *Bioorg. Med. Chem.* **2008**, *16*, 5149–5156; b) M. R. Webb, *Proc. Natl. Acad. Sci. USA* **1992**, *89*, 4884–4887.
- [22] H. Y. Chang, C. C. Chou, M. F. Hsu, A. H. Wang, *J. Biol. Chem.* **2014**, *289*, 18719–18735.
- [23] A. Wissner, *Synthesis* **1979**, *1*, 27–28.
- [24] L. Maier, H. Sporri, *Phosphorus Sulfur Silicon Relat. Elem.* **1992**, *70*, 39–48.
- [25] A. A. Baykov, O. A. Evtushenko, S. M. Avaeva, *Anal. Biochem.* **1988**, *171*, 266–270.

Received: July 7, 2016

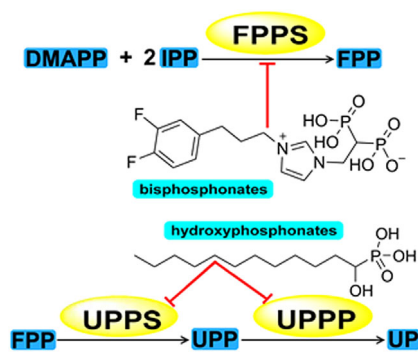
Published online on ■■■■■, 0000

FULL PAPERS

J. Desai, Y. Wang, K. Wang, S. R. Malwal,
E. Oldfield*

■■■ - ■■■

Isoprenoid Biosynthesis Inhibitors Targeting Bacterial Cell Growth



Against the wall: Bisphosphonates inhibit the growth of Gram-negative bacteria (*Acinetobacter baumannii*, *Klebsiella pneumoniae*, *Escherichia coli*, and *Pseudomonas aeruginosa*) at $\sim 1\text{--}4 \mu\text{g mL}^{-1}$ levels, targeting farnesyl diphosphate synthase, whereas monophosphonates inhibit Gram-positive bacteria (*Staphylococcus aureus* and *Bacillus subtilis*) by targeting undecaprenyl diphosphate synthase and undecaprenyl diphosphate phosphatase.